Supporting information for

An excimer process induced a turn-on fluorescent probe for detection of ultra-low concentration of mercury ions

Shujing Fang[a], K. M. K. Swamy,[b] Wen-Yan Zan,[c] Juyoung Yoon[b,*], Shudi Liu[a,*]

[a] College of Chemistry and Chemical Engineering, Yantai University, Yantai 264005, PR China

[b] Department of Chemistry and Nanoscience, Ewha Womans University, Seoul, 03760, Korea

[c] Institute of Molecular Science, Shanxi University, Taiyuan, 030006, PR China

E-mail: liushd2018@163.com, jyoon@ewha.ac.kr

Supplemental results

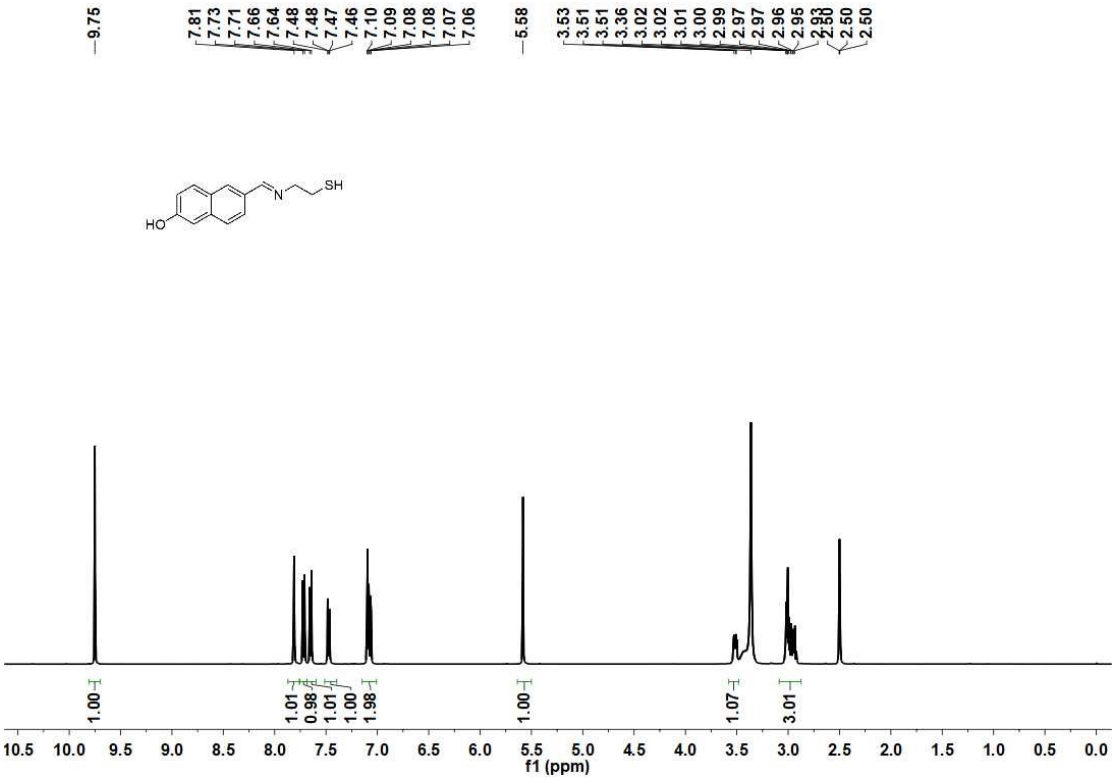

Figure S1 ^{1}H NMR spectrum of probe 1.

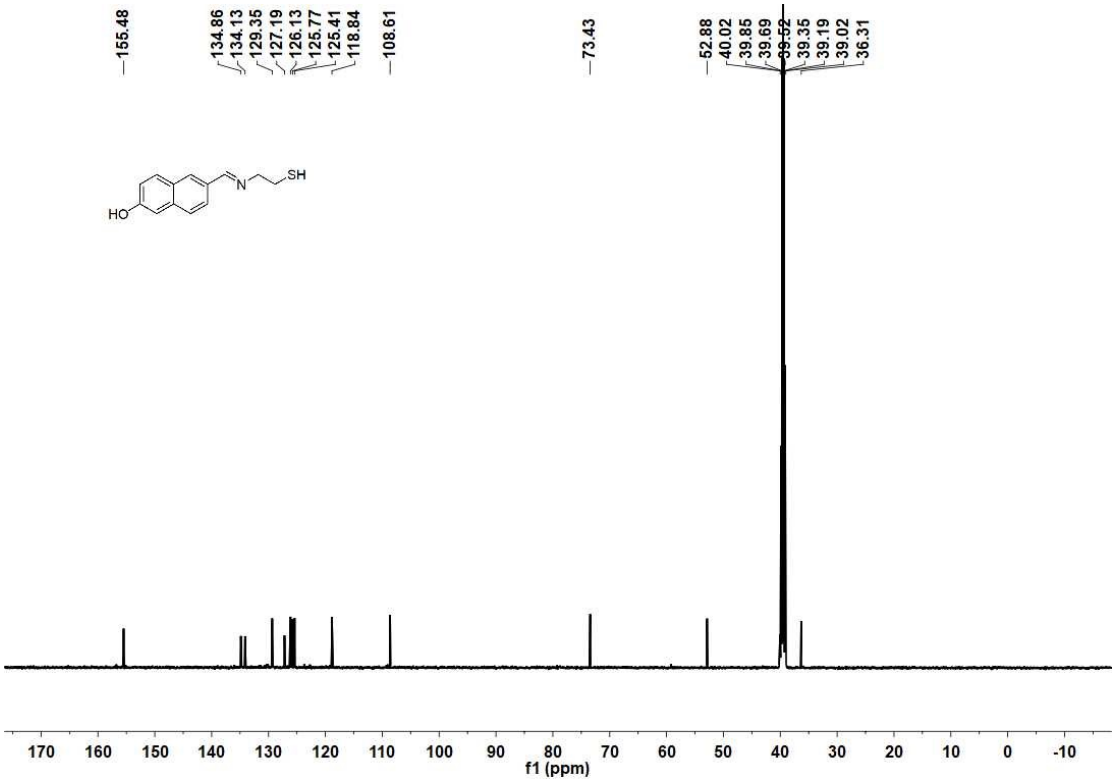

Figure S2 ^{13}C NMR spectrum of probe 1.

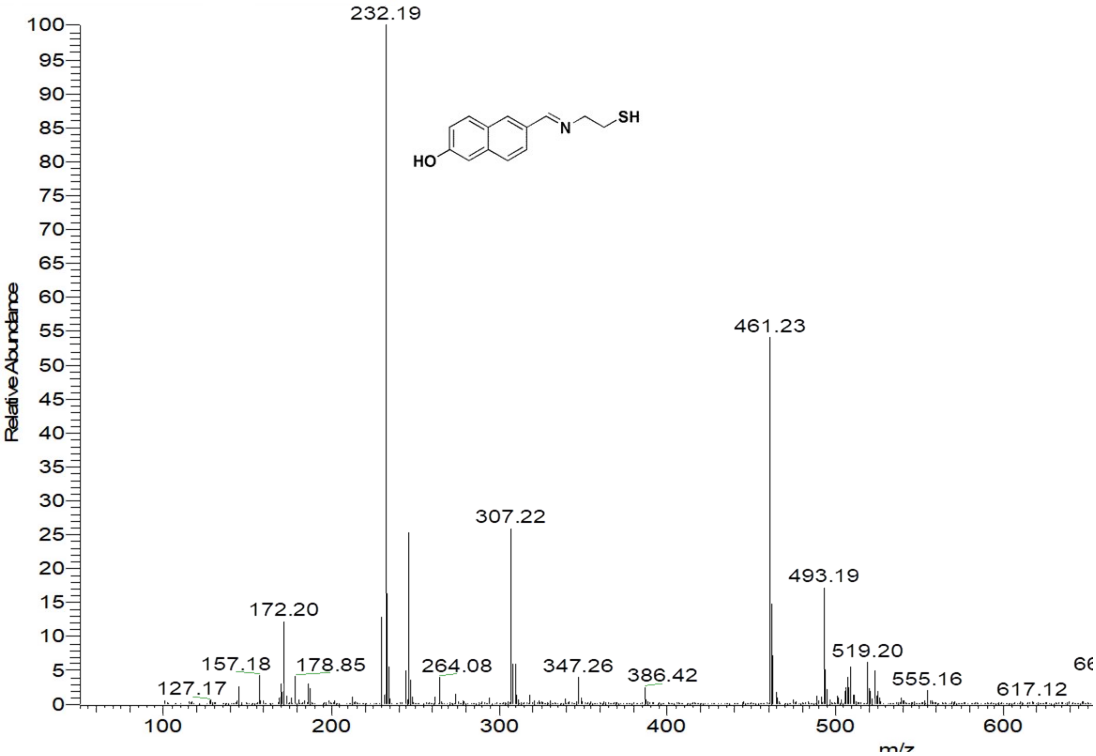

Figure S3 ESI-MS spectrum of probe 1.

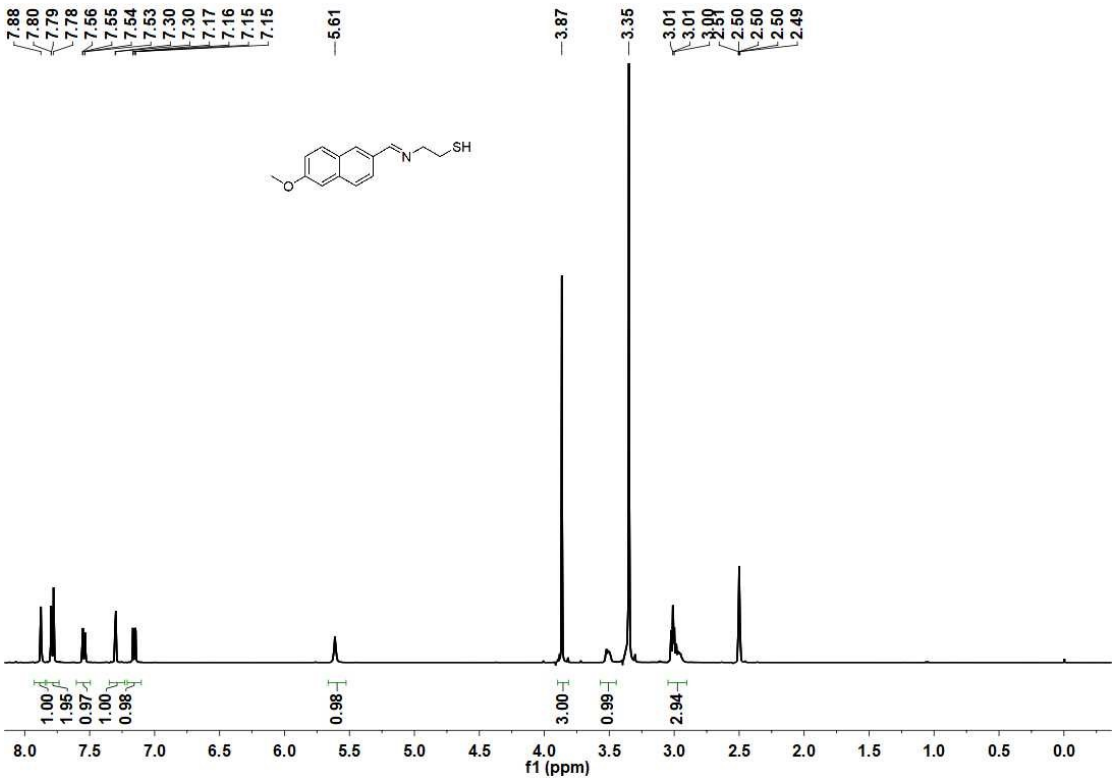

Figure S4 ^{1}H NMR spectrum of probe 2.

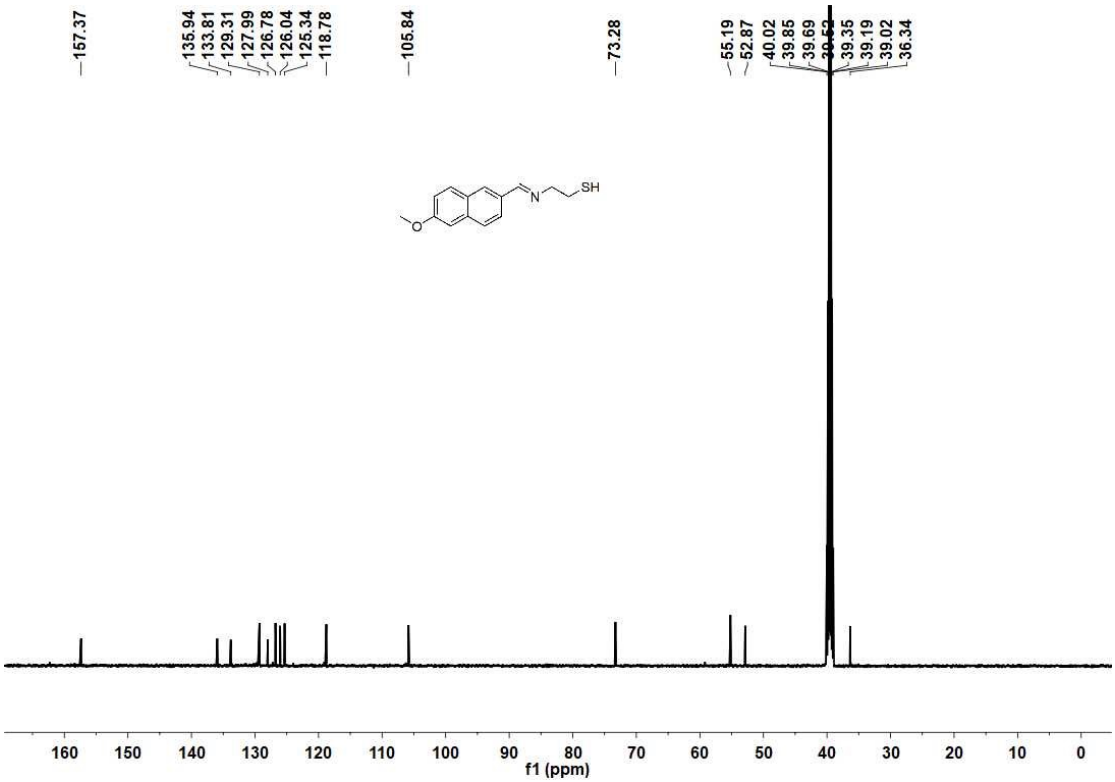

Figure S5 ^{13}C NMR spectrum of probe 2.

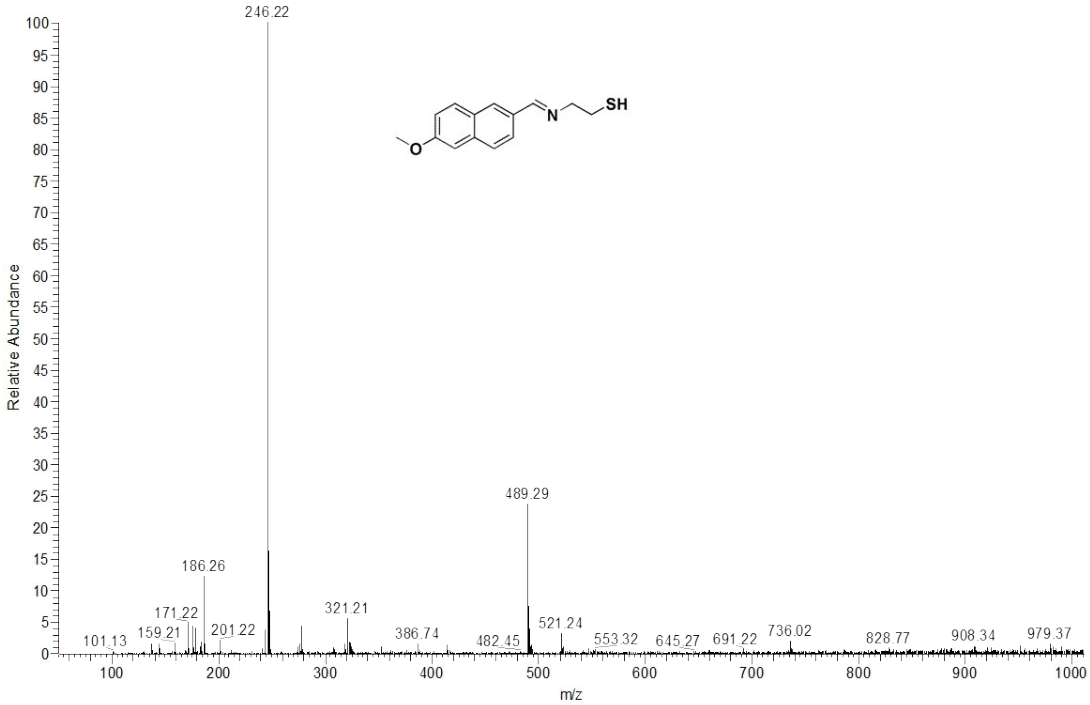

Figure S6 ESI-MS spectrum of probe 2.

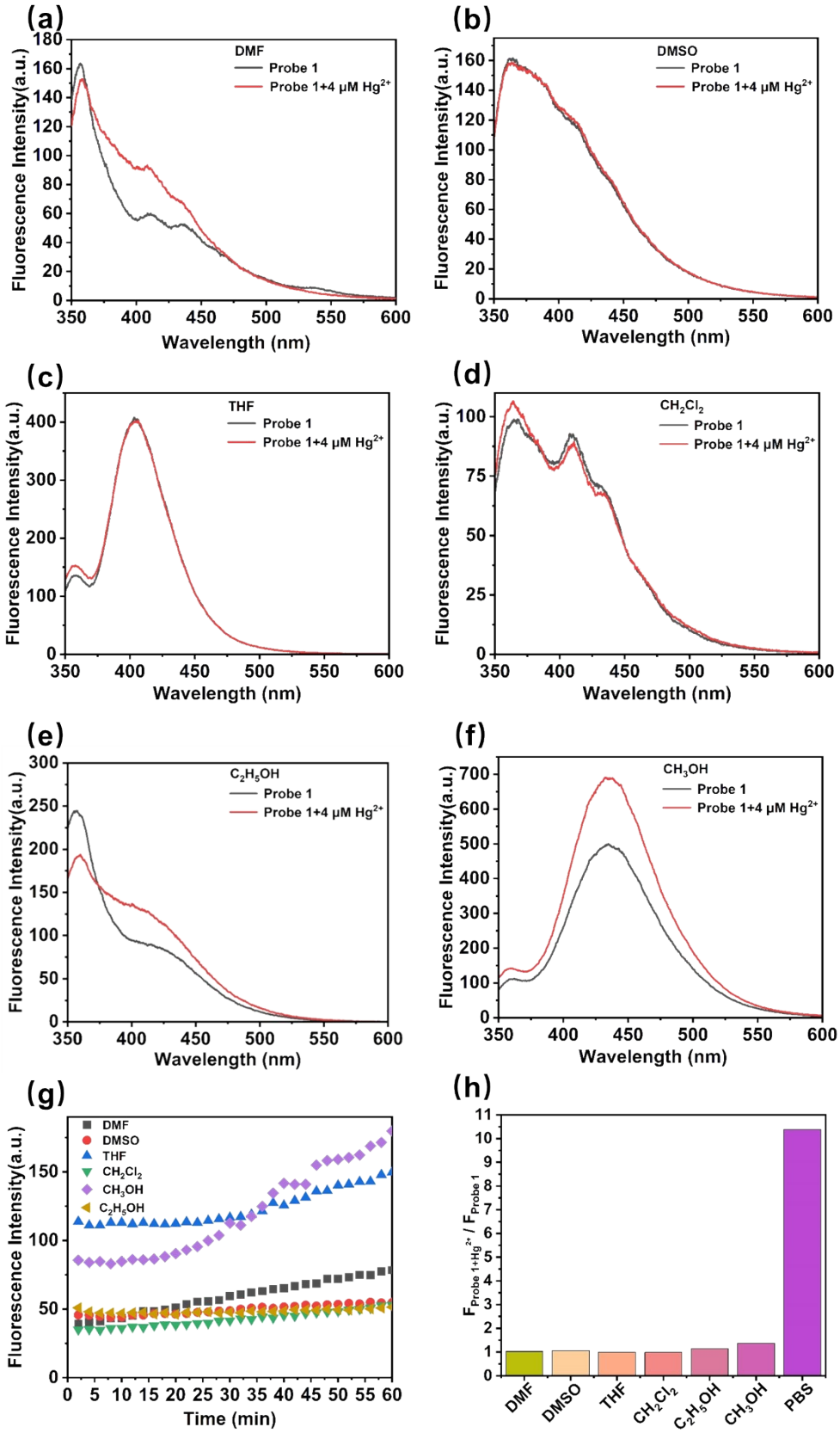

Figure S7 The responses of probe 1 (10 μM) with Hg^{2+} (4 μM) in different solvents. (a) DMF. (b) DMSO. (c) THF. (d) CH_2Cl_2. (e) C_2H_5OH. (f) CH_3OH. (g) time-dependent effects of probe 1 (10 μM)

in different solvents. (h) The ratio of fluorescence intensity in the presence and absence of Hg^{2+}.

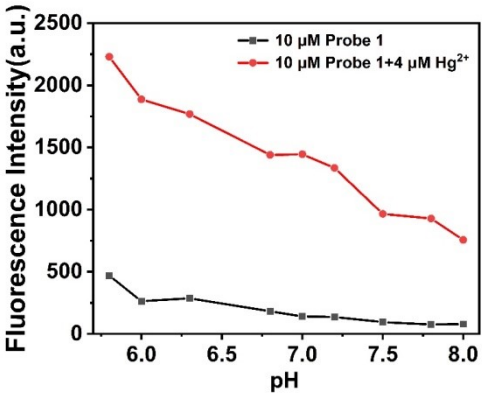

Figure S8 The fluorescence intensities of probe 1 (10 μM) with Hg^{2+} (4 μM) in PBS buffer solution at different pH (5.8 to 8.0).

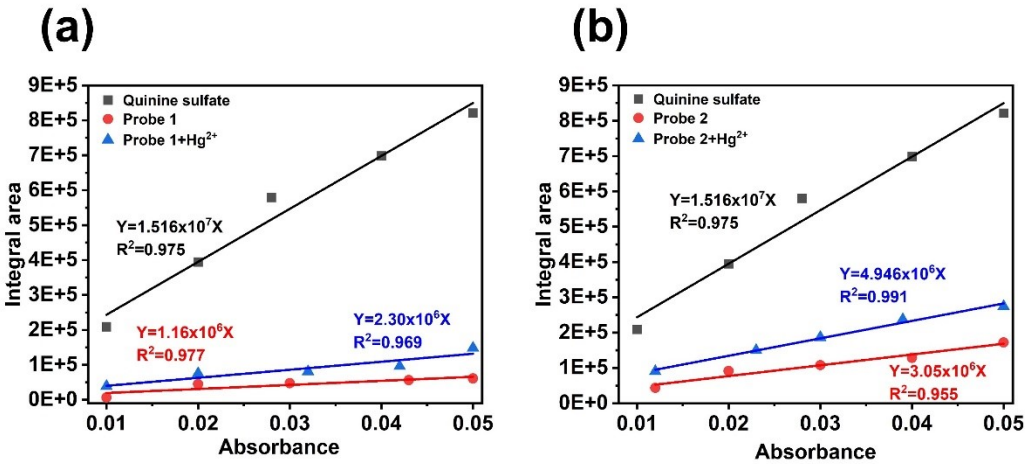

Figure S9 Quantum yields of (a) probe 1 and probe 1 + Hg^{2+}, (b) probe 2 and probe 2 + Hg^{2+} in PBS buffer solution with quinine sulfate (0.54, 0.1 M H_2SO_4) as a reference.

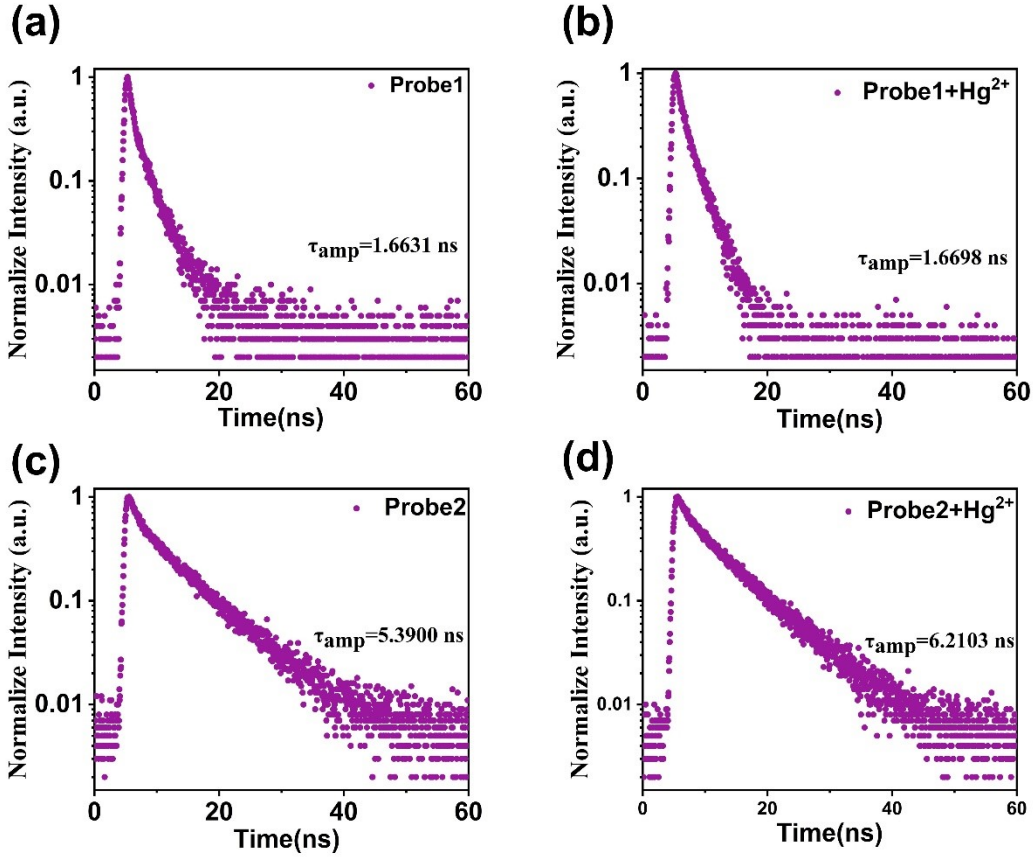

Figure S10 (a, b) Fluorescence lifetimes of probe 1 and probe 1 + Hg^{2+}; (c, d) Fluorescence lifetimes of probe 2 and probe 2 + Hg^{2+}.

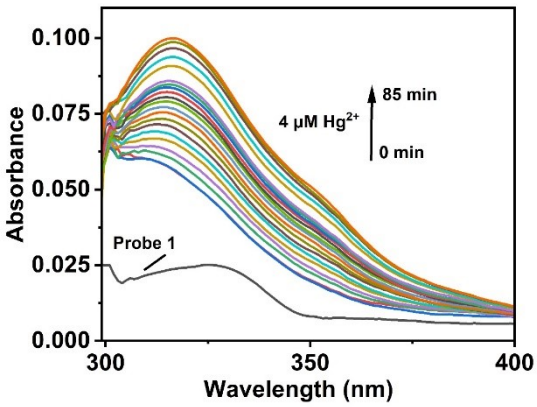

Figure S11 UV-vis spectra of probe 1 (10 μM) in the presence of Hg^{2+} (4 μM) in PBS buffer solution.

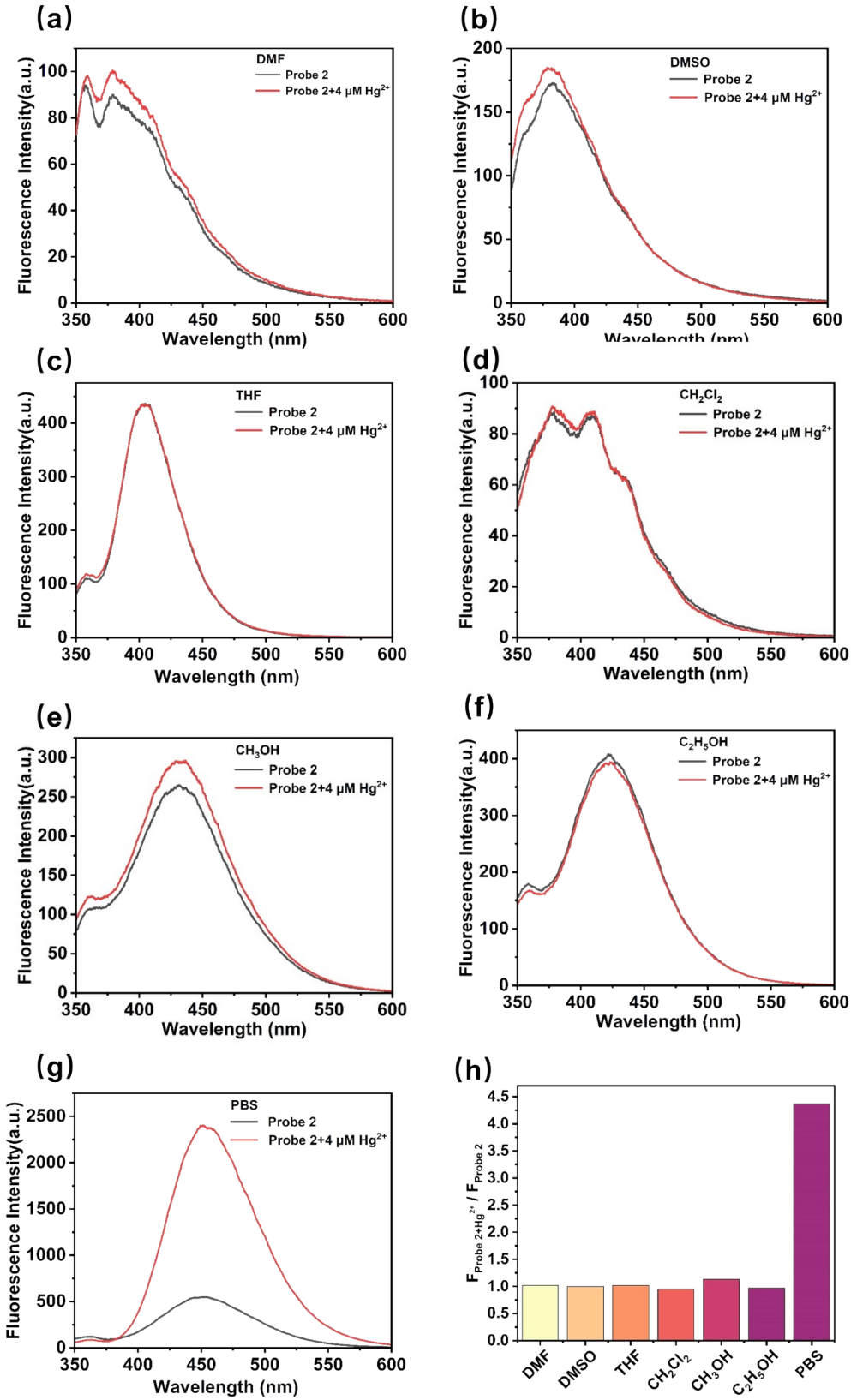

Figure S12 The responses of probe 2 (10 μM) with Hg^{2+}(4 μM) in different solvents. (a) DMF. (b) DMSO. (c) THF. (d) CH_2Cl_2. (e) CH_3OH. (f) C_2H_5OH. (g) PBS. (h) The ratio of fluorescence intensity in the presence and absence of Hg^{2+}.

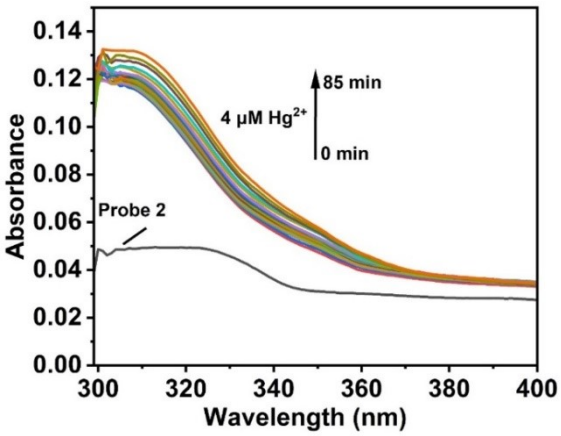

Figure S13 UV-vis spectra of probe 2 (10 μM) in the presence of Hg^{2+} (4 μM) in PBS buffer solution.

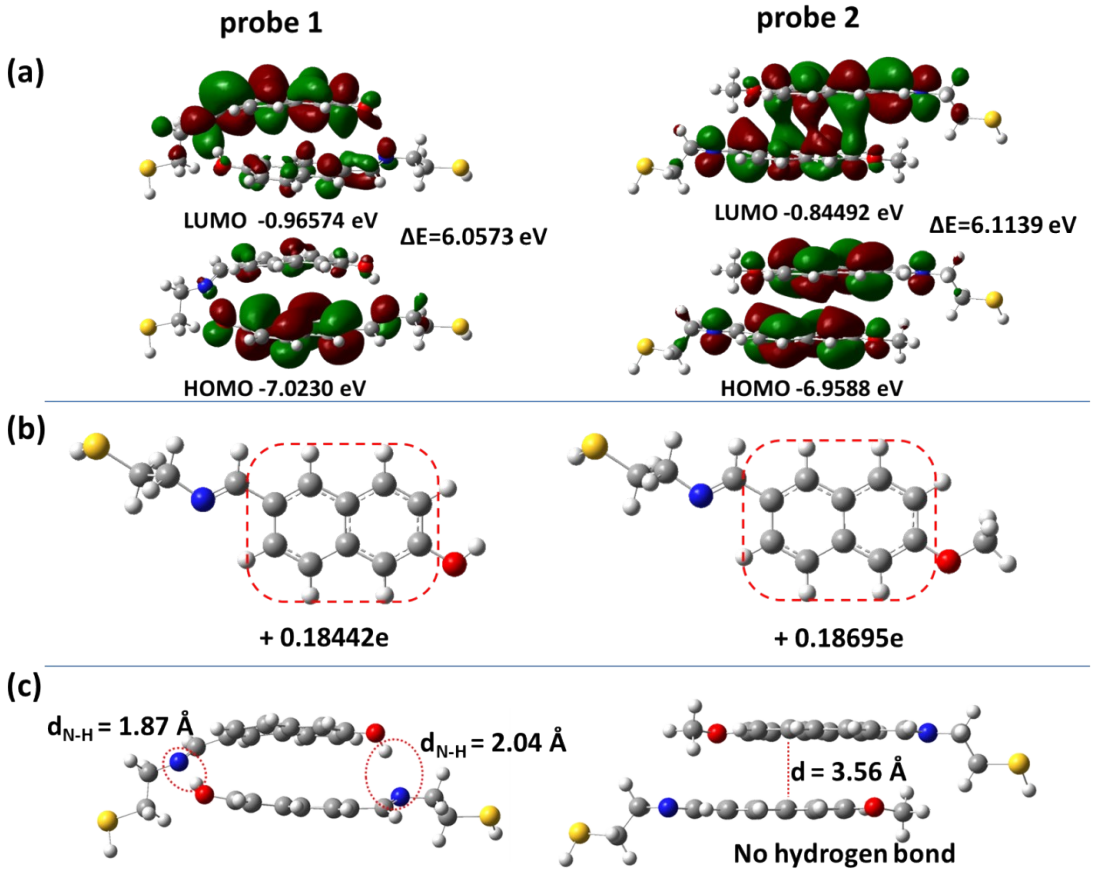

Figure S14 DFT theoretical calculations of probe 1 and probe 2 [1-5]. (a) HOMO and LUNO orbitals of these two probes. (b) The electronic loss abilities of the naphthalene portion in two probes. (c) The π-π stacking mode of two probes.

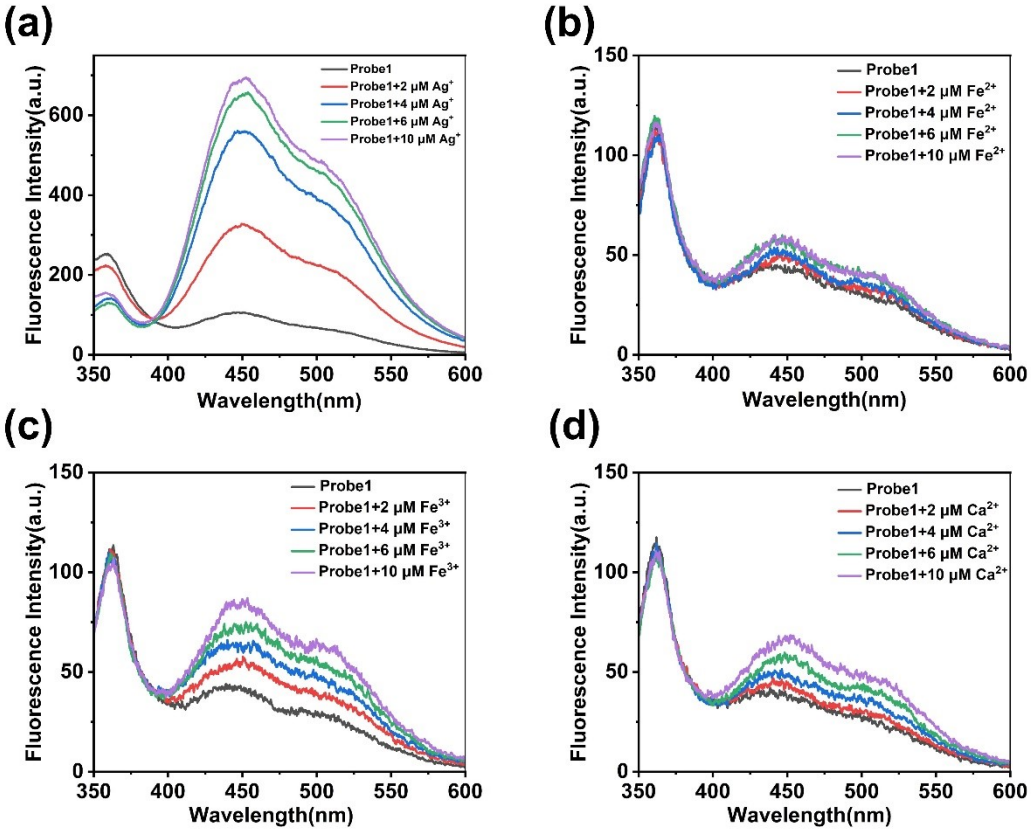

Figure S15 The concentration-dependent fluorescent spectra of probe 1 (10 μM) versus Ag^{+}, Fe^{2+}, Fe^{3+}, Ca^{2+} (0, 2, 4, 6 and 10 μM) in PBS buffer solution.

Table S1: Previous reported fluorescence probes for mercury ion detection.

No.	Probes	Medium	LOD	Applications	Ref.
1	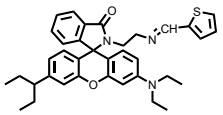	EtOH:H_2O (1:1, v/v)	1 nM	IMTECH No. 3018 cells, water samples	[6]
2	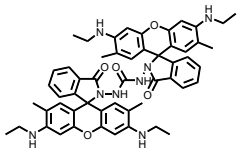	EtOH:H_2O (1:1, v/v)	1.3 nM	L929 cells, animal tissues, plant tissues	[7]
3	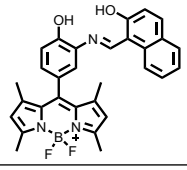	EtOH:Tris–HCl buffer (1:9, v/v)	1.73 nM	HeLa cells, zebrafish, nude mouse	[8]
4	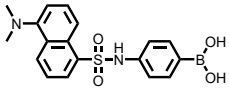 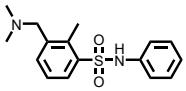	HEPES buffer (1% CH_3CN)	4.02 nM, 1.82 nM	Cells	[9]
5	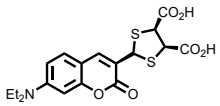	PBS buffer (0.2% DMSO)	2.4 nM	MCF cells	[10]
6	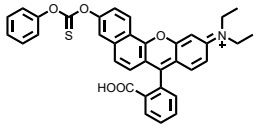	HEPES buffer	3.6 nM	RAW 264.7 macrophage cells, zebrafish, water samples	[11]
7	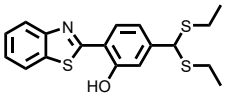	HEPES buffer: EtOH (1: 1, v/v)	5.8 nM	biological serum samples	[12]
8	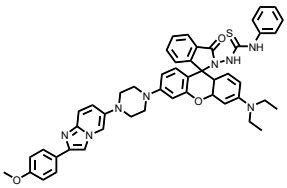	PBS:C_2H_5OH (9/1, v/v)	9.1 nM	Glioma cells, lake water	[13]
9	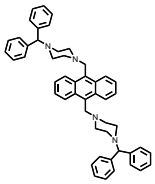	HEPES buffer: ACN (3:7,v/v)	10 nM	HeLa cells, water samples, paper strips, protein medium	[14]
10	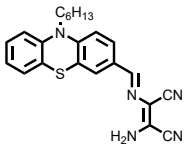	EtOH:H_2O (6:4, v/v)	17.8 nM	HeLa cells	[15]

11	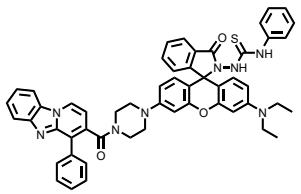	EtOH:H_2O (2:8, v/v)	18.8 nM	Glioma cells	[16]
12	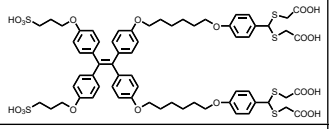	H_2O: THF (1:99, v/v)	20 nM	fibers	[17]
13	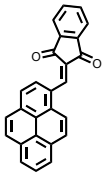	EtOH:H_2O (1:1, v/v)	20.7 nM	water samples	[18]
14	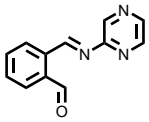	MeOH:H_2O (3:7, v/v)	26.4 nM	HeLa cells,	[19]
15	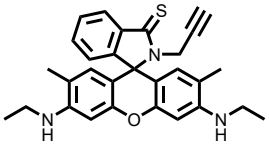	PBS buffer: DMF(8:2, v/v)	39 nM	Cells	[20]
16	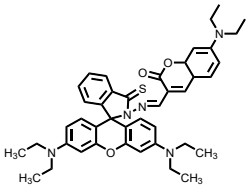	EtOH: Tris–HCl buffer (1:1, v/v)	40 nM	water samples	[21]
17	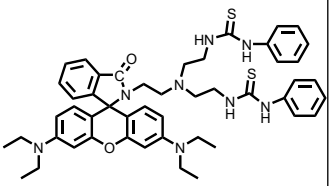	ACN:H_2O (1:99, v/v)	60.78 nM	sf9 cells, water samples	[22]
18	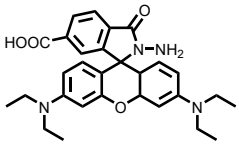	Water	97 nM	HeLa cells, water samples	[23]
19	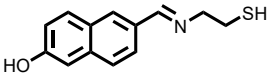	PBS buffer (10 mM)	1.98 nM	water samples, HepG2 cells	This work

Table S2 the atomic charges of C and H on naphthalene portion in probe 1 and probe 2.

probe 1			probe 2		
No.	Atom	Atomic charge	No.	Atom	Atomic charge
1	C	0.30364	1	C	0.30164
2	C	-0.25448	2	C	-0.24045
3	C	-0.02620	3	C	-0.02996
4	C	-0.09386	4	C	-0.09369
5	C	-0.15097	5	C	-0.15083
6	C	-0.27849	6	C	-0.29104
7	H	0.21337	7	H	0.21290
8	H	0.22350	8	H	0.22255
9	C	-0.18524	9	C	-0.18379
10	C	-0.13501	10	C	-0.13416
11	H	0.21370	11	H	0.21199
12	H	0.20984	12	H	0.22011
13	C	-0.12610	13	C	-0.12623
14	C	-0.17100	14	C	-0.17329
15	H	0.20591	15	H	0.20572
16	H	0.23581	16	H	0.23548

References

[1]M. J. FRISCH, G. W. TRUCKS, H. B. SCHLEGEL, et al., Gaussian 16, revision B.01, Gaussian, Inc., Wallingford, CT, 2016.

[2]ZHAO, Y.; TRUHLAR, D. G. The M06 suite of density functionals for main group thermochemistry, thermochemical kinetics, noncovalent interactions, excited states, and transition elements: two new functionals and systematic testing of four M06-class functionals and 12 other functionals. Theor. Chem. Acc. 2008, 120, 215–241.

[3]WEIGEND, F.; AHLRICHS, R. Balanced basis sets of split valence, triple zeta valence and quadruple zeta valence quality for H to Rn: design and assessment of accuracy. Phys. Chem. Chem. Phys. 2005, 7, 3297–3305.

[4]GRIMME, S.; ANTONY, J.; EHRLICH, S.; KRIEG, H. A consistent and accurate ab initio

parameterization of density functional dispersion correction (DFT-D) for the 94 elements H-Pu. J. Chem. Phys. 2010, 132, 154104.

[5] GLENDENING ED, BADENHOOP JK, REED AE, CARPENTER JE, BOHMANN JA, MORALES CM, et al. NBO 5.0/6.0. Madison: Theoretical Chemistry Institute, University of Wisconsin; 2001

[6] MANDAL S, BANERJEE A, LOHAR S, et al. Selective sensing of Hg^{2+} using rhodamine-thiophene conjugate: red light emission and visual detection of intracellular Hg^{2+} at nanomolar level [J]. J. Hazard. Mater., 2013, 261: 198-205.

[7] YANG Y, SHEN R, WANG Y-Z, et al. A selective turn-on fluorescent sensor for Hg (II) in living cells and tissues [J]. Sensor Actuat. B-Chem., 2018, 255: 3479-3487.

[8] XIAO H, LI J, WU K, et al. A turn-on BODIPY-based fluorescent probe for Hg (II) and its biological applications [J]. Sensor Actuat. B-Chem., 2015, 213: 343-350.

[9] NEUPANE L N, PARK J, MEHTA P K, et al. Fast and sensitive fluorescent detection of inorganic mercury species and methylmercury using a fluorescent probe based on the displacement reaction of arylboronic acid with the mercury species [J]. Chem. Commun. (Camb), 2020, 56(19): 2941-2944.

[10] SONG C, YANG W, ZHOU N, et al. Fluorescent theranostic agents for Hg^{2+} detection and detoxification treatment [J]. Chem. Commun. (Camb), 2015, 51(21): 4443-4446.

[11] DUAN Q, ZHU H, LIU C, et al. A carbonothioate-based far-red fluorescent probe for the specific detection of mercury ions in living cells and zebrafish [J]. Analyst, 2019, 144(4): 1426-1432.

[12] ZHOU Y, HE X, CHEN H, et al. An ESIPT/ICT modulation based ratiometric fluorescent probe for sensitive and selective sensing Hg^{2+} [J]. Sensor Actuat. B-Chem., 2017, 247: 626-631.

[13] LI Y, QI S, XIA C, et al. A FRET ratiometric fluorescent probe for detection of Hg^{2+} based on an imidazo[1,2-a]pyridine-rhodamine system [J]. Anal. Chim. Acta, 2019, 1077: 243-248.

[14] SRIVASTAVA P, RAZI S S, ALI R, et al. Selective naked-eye detection of Hg^{2+} through an efficient turn-on photoinduced electron transfer fluorescent probe and its real applications [J]. Anal. Chem., 2014, 86(17): 8693-8699.

[15] VENGAIAN K M, BRITTO C D, SEKAR K, et al. Phenothiazine-diaminomalenonitrile based Colorimetric and Fluorescence “Turn-off-on” Sensing of Hg^{2+} and S^{2-} [J]. Sensor Actuat. B-Chem., 2016, 235: 232-240.

[16] GE Y, LIU A, JI R, et al. Detection of Hg^{2+} by a FRET ratiometric fluorescent probe based on a novel pyrido[1,2-a]benzimidazole-rhodamine system [J]. Sensor Actuat. B-Chem., 2017, 251: 410-415.

[17] ZHAO L, ZHANG Z, LIU Y, et al. Fibrous strips decorated with cleavable aggregation-induced emission probes for visual detection of Hg^{2+} [J]. J. Hazard. Mater., 2020, 385: 121556.

[18] LIANG Q, ZHOU W, WU A, et al. A novel pyrene‐based "off–on" fluorescent probe with high selectivity and sensitivity for Hg^{2+} [J]. J. Chin. Chem. Soc., 2023, 70(10): 1937-1943.

[19] VINOTH KUMAR G G, KESAVAN M P, TAMILSELVI A, et al. A reversible fluorescent chemosensor for the rapid detection of Hg^{2+} in an aqueous solution: Its logic gates behavior [J]. Sensor Actuat. B-Chem., 2018, 273: 305-315.

[20] LIN W, CAO X, DING Y, et al. A highly selective and sensitive fluorescent probe for Hg^{2+} imaging in live cells based on a rhodamine-thioamide-alkyne scaffold [J]. Chem. Commun. (Camb), 2010, 46(20): 3529-3531.

[21] MA Q J, ZHANG X B, ZHAO X H, et al. A highly selective fluorescent probe for Hg^{2+} based on a rhodamine-coumarin conjugate [J]. Anal. Chim. Acta, 2010, 663(1): 85-90.

[22] HONG M, LU X, CHEN Y, et al. A novel rhodamine-based colorimetric and fluorescent sensor for Hg^{2+} in water matrix and living cell [J]. Sensor Actuat. B-Chem., 2016, 232: 28-36.

[23] LI D, LI C Y, LI Y F, et al. Rhodamine-based chemodosimeter for fluorescent determination of Hg^{2+} in 100% aqueous solution and in living cells [J]. Anal. Chim. Acta, 2016, 934: 218-225.